

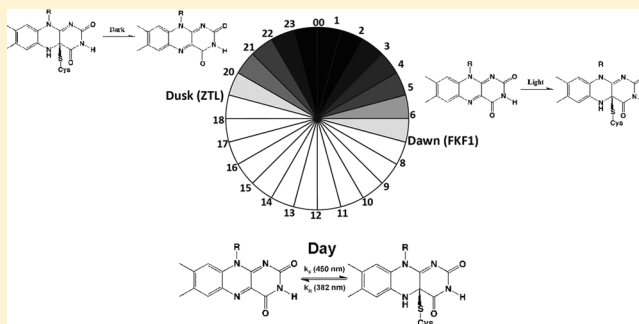
Zeitlupe Senses Blue-Light Fluence To Mediate Circadian Timing in *Arabidopsis thaliana*

Ashutosh Pudasaini and Brian D. Zoltowski*

Department of Chemistry, Southern Methodist University, Dallas, Texas 75275, United States

S Supporting Information

ABSTRACT: Plants employ a variety of light, oxygen, voltage (LOV) domain photoreceptors to regulate diverse aspects of growth and development. The Zeitlupe (ZTL), Flavin-Kelch-Fbox-1 (FKF1), and LOV-Kelch-Protein-2 (LKP2) proteins dictate measurement of the day length, flowering time, and regulation of the circadian clock by blue-light regulation of protein complex formation. Previous reports indicated that ZTL photochemistry was irreversible, which is inconsistent with its role in marking the day–night transition. A kinetic model of LOV domain function predicts that ZTL has evolved unique photochemical parameters to allow it to function as a sensor of environmental light intensity. Moreover, our model indicates that a photocatalyzed reverse reaction is required for the sensitivity of LOV domains to light fluence. Inclusion of a photocatalyzed rate constant allows the establishment of a photostationary steady state of light-activated proteins, whose relative population is sensitive to daily (circadian) or positional (phototropism) oscillations in light intensity. Photochemical characterization confirms that ZTL undergoes adduct decay on a time scale of hours in contrast to previous reports. The fast photocycle allows detection of the day–night transition facilitating circadian timing. ZTL kinetics reflect an evolutionary adaptation of the ZTL/FKF1/LKP2 family to function in distinct aspects of blue-light signaling.



The light, oxygen, voltage (LOV) domain family of proteins is found in prokaryotes and eukaryotes, where they employ small molecule chemistry to sense and adapt to changes in the quality and quantity of blue light. LOV proteins are composed of a core Per-Arnt-Sim (PAS) domain typified by a mixed α/β fold with a central β -scaffold flanked on one side by a series of short helices. The LOV core is coupled to either N- or C-terminal effector domains and harbors a photoreactive flavin [flavin mononucleotide (FMN) or flavin adenine dinucleotide (FAD)] adjacent to a conserved cysteine residue.¹ In this regard, LOV domains impart photodynamic control to a variety of signal transduction elements, such as Ser/Thr kinases, transcription factors, F-boxes, and phosphodiesterases.^{1–4} Recently, they have attracted an increasing level of attention because of their modular nature and ability to be re-engineered in the form of optogenetic tools.⁵ Recent research aimed at improving these optogenetic devices or manipulating cellular signaling has focused on tuning the rate constant of adduct decay to alter photocycle lifetimes.^{6–9} Importantly, how photophysical parameters direct biological function has been quite poorly explored.

LOV domain photochemistry has been well-characterized in several systems. It is defined by blue-light excitation of an oxidized flavin (ground) to induce formation of a cysteinyl-flavin C4a adduct.¹ Upon being returned to darkness, the light state decays to the ground state with kinetics ranging from seconds to days.^{1,9} Interest in the natural variance of LOV domain kinetics has led to the identification of several methods

for modulating the rate of adduct scission in LOV proteins. These include solvent access to the active site,^{6,9,10} hydrogen bonding to the flavin cofactor,^{7,8} and modulation of electron density near the flavin ring.⁹ Through these methods, the rate of adduct decay can be tuned by up to 4 orders of magnitude; however, despite these successes, the biological function of these lifetimes has not been validated. To evaluate the role of LOV adduct-state lifetime in dictating biological responses, we require a system that has evolved distinct photochemical parameters to allow precise timing of biological events.

Such a system exists in *Arabidopsis thaliana*, which has evolved elaborate signaling networks to adjust biological events to changes in the solar day (circadian) and seasonal variations (photoperiodic).^{4,11–14} Importantly, these clock networks are integrated by measurement of the day length, through a family of three LOV domain-containing photoreceptors, Zeitlupe (ZTL), Flavin-Kelch-Fbox-1 (FKF1), and LOV-Kelch-Protein-2 (LKP2).^{4,13–17} This is achieved by the intersection of multiple feedback loops, including a day loop involving FKF1 and an evening loop involving ZTL^{4,11} (Figure 1). Circadian and photoperiodic timing is then achieved by time of day specific function of FKF1 and ZTL. In the day, blue light induces stabilization of FKF1 and ZTL through complexation

Received: July 29, 2013

Revised: September 10, 2013

Published: September 13, 2013



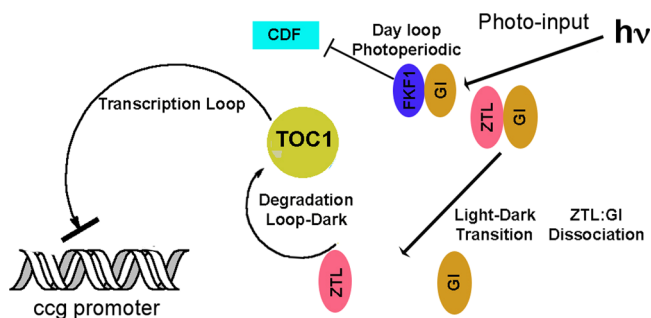


Figure 1. Schematic of circadian and photoperiodic clocks in *A. thaliana*. FKF1 operates in a day loop to regulate photoperiodic timing via degradation of Cycling Dof Factor (CDF). After nightfall, the ZTL–GI complex dissociates and dark-state ZTL targets TOC1 for degradation to repress circadian gene transcription.

with Gigantea (GI).^{16,17} Upon the light–dark transition, the ZTL–GI complex is believed to dissociate to favor interactions with Timing Of Cab expression 1 (TOC1) and subsequent degradation of clock components.¹⁸ Notably, previous characterization of the ZTL/FKF1 family indicated that the lifetime of the light-activated state is on the order of days,¹⁵ thereby limiting the ability of its members to precisely measure the day–night transition. This intriguing paradox begs the questions of how ZTL determines the light–dark transition with kinetics that are not sensitive to that time scale and how LOV domain kinetics are coupled to day-length measurement.

To improve our understanding of circadian and photoperiodic timing in *A. thaliana*, we conducted a comprehensive analysis of the ZTL photocycle. Herein, we report ZTL photocycle kinetics and a simple-yet-elegant model of LOV domain function in fluence-dependent responses. These models provide keen insight into the evolution of photochemical parameters for specific function in biological signaling.

MATERIALS AND METHODS

Cloning and Protein Purification. The nucleotides encoding ZTL and FKF1 were obtained from The *Arabidopsis* Information Resource (Tair).¹⁹ N-Terminal and C-terminal truncations of ZTL and FKF1 were cloned into the pGST-Parallel vector using NcoI and XhoI cut sites. ZTL constructs composed of residues 16–190, 16–165, 29–190, and 29–165 as well as FKF1 28–174 were verified by DNA sequencing (Genewiz). All constructs were expressed in *Escherichia coli* JM109 cells. Cells were grown at 37 °C until an OD₆₀₀ of 0.6 had been achieved. The temperature was then decreased to 18 °C for 40 min, at which point the cells were induced with 0.2 mM isopropyl thiogalactoside (RPI). Cells were harvested after 22 h, pelleted, and stored in 100 mM NaCl, 50 mM Tris (pH 7.4), and 10% glycerol.

ZTL and FKF1 proteins were purified with glutathione affinity resin (Qiagen) at 22 °C. After binding, GST-ZTL and GST-FKF1 were treated on column with 2 mg of TEV protease per milliliter of resin overnight at 4 °C. Proteins were then washed from the column in buffer containing 100 mM NaCl, 50 mM Tris (pH 7.4), and 10% glycerol. An additional round of Ni-NTA chromatography was conducted to remove His₆-TEV. All protein samples were purified using a Superdex S200 size exclusion column equilibrated with 100 mM NaCl, 50 mM Tris (pH 7.4), and 10% glycerol. For Eyring data, protein was purified in 100 mM NaCl, 50 mM Hepes (pH 8.0), and 10% glycerol to avoid the effects of temperature on pH.

UV–Visible Absorbance Spectroscopy and Kinetics.

UV–visible absorbance spectroscopy of ZTL and FKF1 was conducted on either an Agilent 8453 spectrophotometer or a Shimadzu UV-3600 spectrophotometer (Eyring measurements). Spectra were recorded for proteins at a concentration of approximately 30 μM and measured using a 1 cm path-length cuvette at temperatures between 285 and 303 K. All samples were exposed to a broad-spectrum white floodlight source (150 W), while being incubated on ice to populate the light state.

Kinetics of ZTL thermal reversion were obtained from the absorbance at 450 and 478 nm as a function of time. All values for 450 and 478 nm were corrected for deviations in the baseline by subtracting the absorbance at 600 nm. Full spectra were collected at varying times, such that a minimum of 10 data points per half-life was obtained. To validate that the sample procedure did not affect kinetic measurements, the rate of data acquisition was varied along with removal of a UV component of the light source (Figure S1 of the Supporting Information). Absorbance spectra were obtained at these time points via ~0.5 s exposures from the 8453 deuterium and tungsten light sources. Data were fit using mono- and biexponential equations as required to extract kinetic parameters (see Figure S2 of the Supporting Information). All time constants are reported as 1/ $k_{\text{adduct scission}}$ that is averaged between the values obtained at 450 and 478 nm. Solvent isotope effect ($\text{SIE} = k_{\text{H}_2\text{O}}/k_{\text{D}_2\text{O}}$) measurements were made by first transferring the protein into buffer containing 95% D₂O prior to data collection.

The solvent accessibility of the active site was assayed by analyzing the ability of imidazole to catalyze adduct scission. Stock solutions containing 950 mM imidazole in 100 mM NaCl, 50 mM Tris (pH 8.0), and 10% glycerol were prepared. Samples of ZTL were then diluted to a concentration of 30 μM and contained 10, 50, 100, 150, 175, and 200 mM imidazole. Kinetics of imidazole catalysis were calculated as described above. A solvent accessibility factor (a) was calculated using methods published previously.²⁰ Briefly

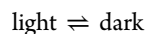
$$\text{rate} = a(k[\text{adduct}][\text{base}]) \quad (1)$$

The slope of a plot of k versus base concentration is equivalent to

$$\frac{\text{slope}}{[\text{adduct}]} = a \quad (2)$$

The slope was calculated using the concentrations of both protein and imidazole in units of molarity. All calculations were made with a protein concentration of 30 μM.

Derivation of Kinetic Models. Our kinetic model was modified from that of Kottke et al.²¹ We consider the general reversible reaction



where light refers to the light state of the protein harboring a cysteinyl C4a adduct. The return to the resting dark state can proceed through either a thermal process or a photochemical process. This results in three chemical pathways influencing the relative population of the light and dark states of LOV proteins.

Rate of adduct decay: thermal

$$\frac{d[\text{light}]}{dt} = -k_T[\text{light}] \quad (3)$$

Rate of adduct decay: photochemical

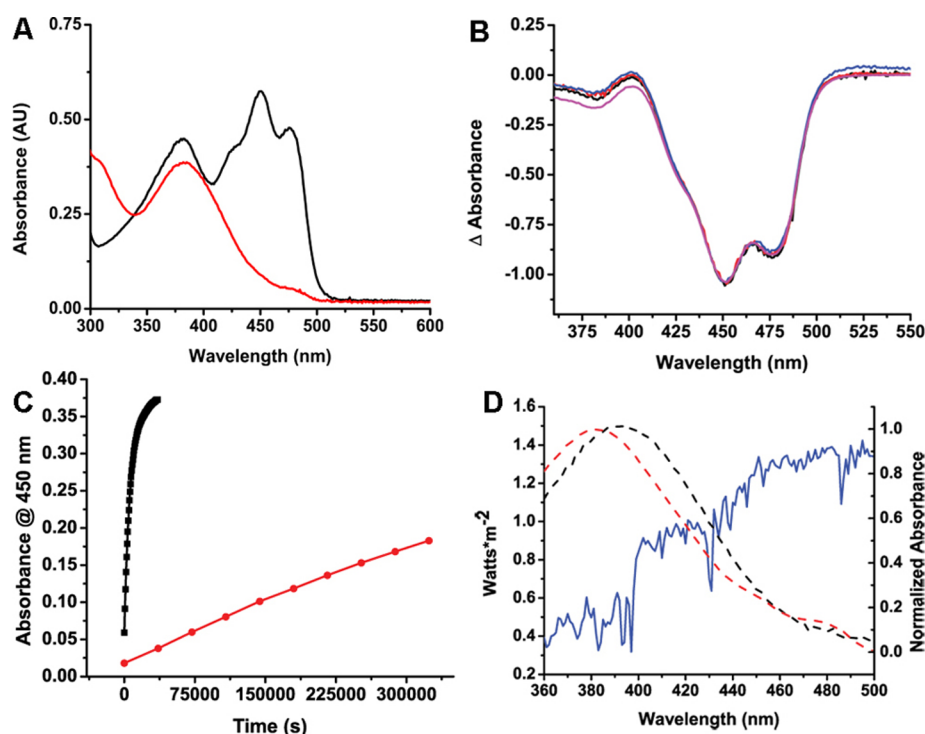


Figure 2. ZTL photochemistry. (A) Dark-state (black) and light-state (red) spectra of ZTL. (B) Light–dark difference spectra of ZTL residues 16–165 (black), 29–165 (red), 29–190 (blue), and 16–190 (magenta). All constructs bear similar differences following photoillumination. (C) Differences between ZTL and FKF1 kinetics. The absorbance at 450 nm returns on a rapid time scale for ZTL (black) compared to FKF1 (red); proteins are shown at equivalent concentrations. (D) Light-state spectra of ZTL (red) compared to those of VVD (black). The blue shift in ZTL light-state spectra results in a decreased level of spectral overlap with solar flux,²³ $F(\lambda)$ (blue). A subtle 10 nm blue shift in the light-state peak has potential effects on cellular signaling. The decreased k_R in the model using VVD spectra (black) results in a decrease in the light:dark ratio at all fluences compared to that of our model with the ZTL spectra (red).

$$\frac{d[\text{light}]}{dt} = -k_R[\text{light}] \quad (4)$$

Rate of adduct formation: photochemical

$$\frac{d[\text{light}]}{dt} = k_F[\text{dark}] \quad (5)$$

Thus, the overall rate can be defined as

$$\frac{d[\text{light}]}{dt} = k_F[\text{dark}] - (k_R + k_T)[\text{light}] \quad (6)$$

Using the steady-state approximation, we obtain

$$(k_R + k_T)[\text{light}] = k_F[\text{dark}] \quad (7)$$

Which allows us to define the [light]:[dark] ratio as

$$\frac{[\text{light}]}{[\text{dark}]} = \frac{k_F}{k_T + k_R} \quad (8)$$

We can define k_F and k_R in terms of fluence rate $F(\lambda)$, absorption cross section $\sigma(\lambda)$, and the quantum yields of adduct formation and scission, ϕ_F and ϕ_R , respectively. For ϕ_F and ϕ_R , we used estimates derived from other systems: $\phi_F = 0.5$ ^{9,22} and $\phi_R = 0.30$.²² For $F(\lambda)$, we use a 360–500 nm spectral window and standard total irradiance data from ASTM.²³ We thus define k_R and k_T by the following expressions:

$$k_R = \phi_R \int_{360 \text{ nm}}^{500 \text{ nm}} F(\lambda) \sigma_R(\lambda) d\lambda \quad (9)$$

$$k_F = \phi_F \int_{360 \text{ nm}}^{500 \text{ nm}} F(\lambda) \sigma_F(\lambda) d\lambda \quad (10)$$

Combining eqs 5, 7, and 8, we can predict the relative populations of light and dark states of LOV domain-containing photoreceptors under physiologically relevant actinic flux.

$$\frac{[\text{light}]}{[\text{dark}]} = \frac{\phi_F \int_{360 \text{ nm}}^{500 \text{ nm}} F(\lambda) \sigma_F(\lambda) d\lambda}{k_T + \phi_R \int_{360 \text{ nm}}^{500 \text{ nm}} F(\lambda) \sigma_R(\lambda) d\lambda} \quad (11)$$

RESULTS

Previous studies of ZTL, FKF1, and LKP2 indicated that the family has unusually long photocycles that did not recover on the time scale of protein stability.¹⁵ Later studies indicated that FKF1 did indeed return to the dark state, but with a half-life of 62 h. They deemed that the long recovery of FKF1 in part results from the insertion of a loop between helices E and F.²⁴ Such a long lifetime is ideal for activation at first light (night–day transition) but cannot allow function at dusk (ZTL) because of the prolonged population of the light state. Thus, if ZTL has a lifetime equivalent to that of FKF1, other factors must accelerate ZTL turnover in a light-dependent manner, or the current characterization of ZTL is incomplete.

Several factors indicate ZTL photochemistry may have evolved distinctly from FKF1 photochemistry to function at the day–night transition. First, the long lifetime of ZTL is based on comparisons to FKF1 and LKP2, as direct analysis of ZTL was complicated by the instability of the protein.¹⁵ Second, ZTL mutants exhibit a fluence-dependent effect on

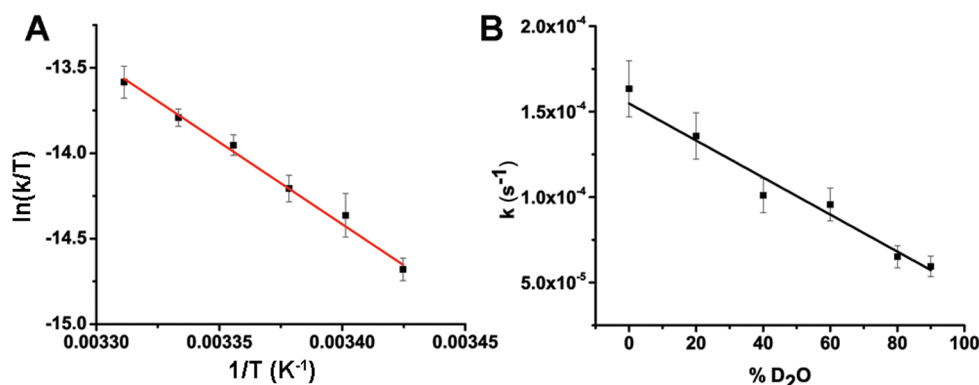


Figure 3. Thermodynamics and SIE analysis of Zeitlupe. (A) The Eyring plot of ZTL demonstrates a weak temperature dependence, with a ΔH^\ddagger of 78 kJ/mol and an entropy of activation of $-50 \text{ J mol}^{-1} \text{ K}^{-1}$. (B) The proton inventory method indicates a linear dependence of the rate of adduct decay, consistent with a single proton transfer event being rate-limiting. Error bars are depicted as $\pm 10\%$, which reflects errors in sample construction.

circadian period, resulting in a maximal circadian period of 36 h under low-light (LL) conditions ($0.6\text{--}8 \mu\text{mol m}^{-2} \text{ s}^{-1}$).²⁵ Above $8 \mu\text{mol m}^{-2} \text{ s}^{-1}$, the circadian period collapses to near wild type (WT) (28 h), indicating ZTL circadian function may be limited to LL conditions. Third, ZTL proteins are destabilized in the dark, resulting in a 4-fold decrease in protein levels.¹³ Thus, if no additional factors regulate ZTL stability, its photocycle must proceed with a lifetime of $<4 \text{ h}$ to allow for two half-lives following nightfall (4-fold decrease in protein levels). For these reasons, we conducted a comprehensive study of ZTL photochemistry.

Secondary structural predictions of ZTL indicate the presence of N- and C-terminal helices that flank the core LOV domain. Because N- and C-terminal elements are important for signaling in other LOV proteins and can affect the kinetics of adduct scission,^{20,26–28} ZTL constructs that contain the LOV core (residues 29–165), an N-terminal helix (residues 16–165), a C-terminal helix (residues 29–190), and both N- and C-terminal helices (residues 16–190) were prepared. Kinetic characterization of all constructs and FKF1 indicates that ZTL photochemistry has indeed evolved unique photochemical kinetics distinctly different from those of FKF1. Spectral analysis of ZTL and FKF1 indicates the presence of bound oxidized FMN under dark-state conditions. Illumination with blue light results in rapid bleaching of the FMN chromophore and formation of a 382 nm light-absorbing intermediate (Figure 2), consistent with formation of a cysteinyl-flavin C4a adduct.¹ ZTL and FKF1 both undergo spontaneous adduct scission under dark-state conditions with markedly different kinetics. ZTL reverts to the ground state rapidly ($\tau = 1.7 \text{ h}$) compared to FKF1 ($\tau > 100 \text{ h}$). Notably, the difference in kinetics may facilitate differential function of ZTL (light–dark transition) and FKF1 (day loop).

Analysis of ZTL photochemistry reveals several aspects not expected from previous LOV domain studies. First, the presence of FMN instead of FAD is consistent with previous reports¹⁵ but is surprising. Sequence analysis indicates the presence of an insertion between helices E and F. The loop insertion is responsible for accommodating the FAD side chain in other circadian clock photoreceptors.^{28,29} On the basis of analogy to Vivid and White-Collar-1, it was predicted that ZTL, FKF1, and LKP2 would bind FAD.²⁹ The absence of FAD indicates the loop insertion may be involved in alternative aspects of LOV domain function, such as tuning photochemical

parameters or mediating a biological signal. Second, examination of the spectral characteristics of ZTL constructs indicates factors important for LOV domain function. The ZTL ground-state spectrum is composed of two broad absorption peaks. The lower-energy $S_0\text{--}S_1$ transition is centered at 450 nm, with vibrational bands at 425 and 475 nm. The UV-A ($S_0\text{--}S_2$) absorption band is blue-shifted compared to those of other LOV proteins (382 nm) with no vibrational fine structure. Whereas the spectral characteristics of ground-state ZTL are similar to those of other LOV proteins, the absorption spectrum of the light state differs. The adduct-state peak mirrors the 382 nm dark-state absorption band with a slight decrease in the extinction coefficient (Figure 2A). This results in a considerable blue shift of the adduct state compared to other LOV proteins (Figure 2D). Shifts in the UV-A transition are known to be sensitive to solvent polarity and H-bonding interactions in the active site.⁷ Large blue shifts of the adduct state have been seen in some variants of YtvA where H-bonding interactions to FMN are altered.⁷ However, no biological functions of spectral shifts in LOV domain spectra have been identified. To improve our understanding of ZTL photochemistry, we performed a comprehensive analysis of the ZTL photocycle.

The temperature dependence of reaction kinetics can yield a distinct understanding of the reaction landscape for adduct scission.⁸ Eyring analysis of the ZTL photocycle reveals factors that mediate proper function in a circadian clock (Figure 3A). First, ZTL reversion proceeds with a weak temperature dependence because of a low enthalpy of activation (78 kJ/mol). Notably, the ΔH^\ddagger is comparable to that of the fast-cycling isolated LOV domain of EL222 (75 kJ/mol) despite a slower rate of adduct decay (1.7 h for ZTL and 22 s for the LOV domain of EL222).⁸ Other LOV proteins with comparable adduct-state lifetimes typically have ΔH^\ddagger values exceeding 100 kJ/mol.⁷ The low ΔH^\ddagger is compensated by a large unfavorable ΔS^\ddagger ($-50 \text{ J mol}^{-1} \text{ K}^{-1}$), thereby maintaining a moderate rate of adduct decay but minimizing the temperature dependence of the reaction rate. The low ΔH^\ddagger in ZTL reduces the need for large compensatory factors to maintain the temperature independence of the circadian clock. Importantly, similar entropic compensation was observed in variants of YtvA that altered the H-bonding properties of residues interacting with the flavin cofactor.⁷

The weak H-bonding interactions identified in the Eyring data and spectral profiles may impact ZTL signaling or photocycle mechanism. A key step in signaling and adduct decay involves H-bonding interactions with the N5 position of the isoalloxazine ring that is believed to facilitate transfer of the N5 proton to a currently unidentified base.⁹ As altered H-bonding interactions may perturb this mechanism, the ZTL photocycle was probed for identification of the rate-limiting step of adduct decay and the effect of small molecule bases.

ZTL was probed using the proton inventory technique to identify the rate-determining step of adduct scission in ZTL. Proton inventory experiments reveal that ZTL maintains a primary solvent isotope effect (SIE = 2.7), consistent with abstraction of a proton from N5 being rate-limiting (Figure 3B). Moreover, the dependence of the rate constant with respect to D₂O concentration is linear, reflecting the fact that a single proton is involved in the rate-determining step of the reaction (Figure 3B).

Consistent with N5 deprotonation being rate-limiting, ZTL kinetics are sensitive to the presence of external small molecule bases such as imidazole. Previous studies have suggested that imidazole acts in the vicinity of the N5 proton or through a network of H-bonding interactions to catalyze scission of the cysteinyl-C4a adduct.^{9,30} The dependence of the rate constant on imidazole concentration can inform the relative solvent accessibility of the active site, which can be quantified in terms of a protection factor, *a*.²⁰ Here large values of *a* reflect a high degree of solvent accessibility or a highly coupled H-bonding network. Consistent with the data described above, ZTL has a low protection factor (*a* = 53) compared to those of other LOV domain-containing proteins (Figure S3 of the Supporting Information and Table 1). The protection factor for ZTL is

Table 1. Solvent Accessibility of ZTL and Other LOV Proteins^a

protein	rate (s ⁻¹)	τ (s)	accessibility constant, <i>a</i> (×10 ⁴)
ZTL	1.6 × 10 ⁻⁴	6200	0.0053
EL222 ^b	3.4 × 10 ⁻²	29	0.25
EL222 A79Q ^b	4.4 × 10 ⁻³	227	0.018
VVD ^c	5.6 × 10 ⁻⁵	18000	0.0094
VVD I74V ^c	1.4 × 10 ⁻³	730	0.010
VVD I74V/I85V ^c	3.5 × 10 ⁻²	28	200
LOVK (1–163) ^d	2.2 × 10 ⁻⁴	4500	4.5
LOVK (1–138) ^d	8.3 × 10 ⁻³	120	163.6

^aThe dependence of rate constants on the concentration of imidazole allows determination of a solvent accessibility constant, *a* (eqs 1 and 2). The solvent accessibility of ZTL is similar to those of other circadian clock photoreceptors (VVD) but weaker than those of other bacterial LOV proteins. ^bEL222 data obtained from ref 8. ^cVVD data obtained from ref 9. ^dLOVK data obtained from ref 20.

similar in magnitude to those of other circadian clock photoreceptors (*a* = 94 for VVD) and significantly smaller than those of bacterial stress response proteins (*a* = 2500 for EL222, and *a* = 45000 for LOVK) (Table 1). Notably, the protection factor of ZTL is similar in magnitude to those of even fast cycling variants of VVD (*a* = 100 for I74V), indicating solvent access may not be the predominant factor dictating the lifetime of adduct scission in ZTL. Rather, the low protection factor likely reflects alteration of H-bonding interactions.

Importantly, although H-bonding interactions have been shown to modulate photocycle kinetics in LOV domain

mutants^{7–9} and the tunability of LOV proteins has been realized in artificial systems,^{7–9,31} a keen role in photocycle parameters affording biological advantages has not been observed. In *A. thaliana*, ZTL plays a pivotal role in marking the day–night transition. In concert with FKF1, this allows precise timing of seasonal variations in day length, thereby facilitating circadian and photoperiodic timing. To determine the role of LOV domain photochemical parameters in dictating biological function, we have developed a simple kinetic model to examine the effect of LOV domain chemistry on determining fluence-based responses.

Kinetic Model of LOV Domain Function. LOV domain chemistry has been studied well in many systems. Although several mechanisms of adduct formation and disruption have been proposed, the most likely reaction process involved blue-light excitation to an excited triplet state.³² Adduct formation then proceeds through proton-coupled electron transfer from the active-site cysteine to the N5 position of the isoalloxazine ring, followed by rapid radical recombination between the Cys radical and the C4a position.^{1,32} Once populated, the C4a adduct (light state) can decay to the ground state via one of two pathways: (1) light-stimulated adduct scission²² and (2) thermal recovery. The presence of a light-stimulated pathway results in rapid formation of a photostationary state that can be defined by

$$\frac{[\text{light}]}{[\text{dark}]} = \frac{k_F}{k_T + k_R} \quad (8)$$

where *k_F* is the rate constant for adduct formation, *k_R* the rate constant for light-stimulated adduct decay, and *k_T* the rate constant for thermal decay. The light:dark (L:D) ratio then defines the relative concentration of LOV domains in the activated light state compared to the concentration that remains inactive (dark state). This ratio reflects the relative degree of activation for a given cellular pool of LOV proteins. Notably, *k_F* and *k_R* can be determined from fluence rate *F*(λ), absorption cross section σ(λ), and the quantum yields of adduct formation and scission, φ_F and φ_R, respectively.

$$k_R = \phi_R \int_{360 \text{ nm}}^{500 \text{ nm}} F(\lambda) \sigma_R(\lambda) d\lambda \quad (9)$$

$$k_F = \phi_F \int_{360 \text{ nm}}^{500 \text{ nm}} F(\lambda) \sigma_F(\lambda) d\lambda \quad (10)$$

Previous studies of LOV domain function have focused exclusively on tuning the thermal pathway to affect biological function or improve optogenetic tools.^{6,7,9,31} This in part is due to the fact that a biological function of the photoinitiated adduct decay has not been observed. To evaluate the significance of *k_R*, we examined the steady-state L:D ratio as a function of actinic flux in the presence and absence of *k_R*. This allowed us to view the relative concentrations of active (light) to inactive (dark) LOV proteins as a function of environmental light intensity. Allowing *k_R* to be reduced to 0 results in one of two conditions. Under high flux (600 μmol m⁻² s⁻¹), even the fastest-cycling LOV proteins reach light-state populations exceeding 80% (Figure 4A). Such conditions imply that daytime lighting conditions are sufficient to saturate all currently identified LOV proteins. In contrast, under low flux (20 μmol m⁻² s⁻¹), only the slowest-cycling LOV proteins reach a light-state population exceeding 10% (Figure 4B). Thus, fast-cycling LOV proteins such as phototropins would require

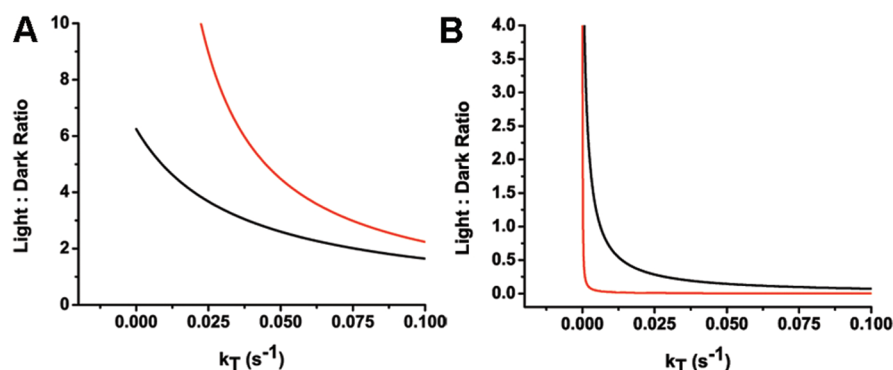


Figure 4. Biological relevance of photoinitiated adduct decay. Relative concentrations of the light state compared to the dark state (L:D ratio) as a function of k_T in the presence (black) and absence (red) of the photoinitiated reverse reaction. (A) High-light conditions (HL, fluence rate of $600 \mu\text{mol m}^{-2} \text{s}^{-1}$). (B) Low-light conditions (LL, fluence rate of $20 \mu\text{mol m}^{-2} \text{s}^{-1}$). In both, inclusion of the k_R term broadens the dynamic range of the L:D ratio, allowing sensitivity to blue-light fluence.

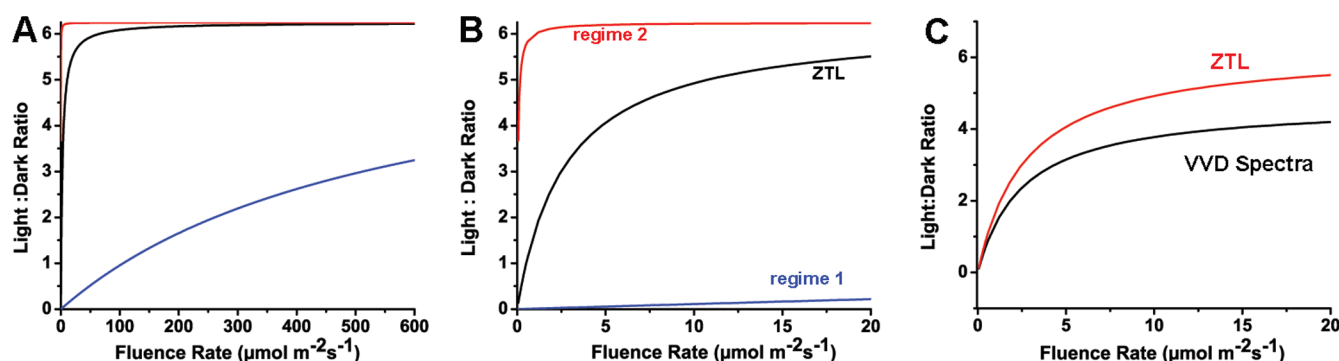


Figure 5. Light:dark ratios as a function of fluence rate. The sensitivity of a LOV domain to the L:D ratio is dependent on k_T . Large k_T values (blue, $k_T = 0.033$, regime 1) are sensitive across the entire fluence range, whereas FKF1-like photochemistry (red, $k_T = 2.5 \times 10^{-6}$, regime 2) is always activated under physiological light conditions. An intermediate regime is occupied by ZTL photochemistry (black, $k_T = 1.6 \times 10^{-4} \text{s}^{-1}$), allowing ZTL to be sensitive to dawn–dusk conditions. (A) Entire dynamic range of the fluence rate. (B) Sensitivity to the low-light fluence range. (C) Effects of the light-state absorption profile on the light:dark ratio. A subtle 10 nm blue shift in the light-state peak has potential effects on cellular signaling. The decreased k_R in the model using a VVD-like spectrum (black) results in a decrease in the light:dark ratio at all fluences compared to our model with the ZTL spectrum (red).

extensive amplification of light-state signals to function under these conditions and would be limited in their ability to distinguish fluence intensities under low-flux conditions. This contradicts known biological data, where phototropins exhibit biological responses at fluences as low as $1 \mu\text{mol m}^{-2} \text{s}^{-1}$.³³ Thus, if photoinitiated adduct decay is neglected, LOV domain photochemistry is reduced to sensing lights on and off as opposed to flux gradients as required for processes such as phototropism.

Inclusion of k_R results in an altered relationship between actinic flux and k_T . Here, the position of the photostationary state is dictated by the relative values of k_R and k_T . Under both low-light (LL) and high-light (HL) conditions, we observed broadening of the L:D ratios relative to k_T (Figure 4). As such, inclusion of k_R allows LOV proteins to be sensitive to environmental flux over the range of naturally observed k_T values, thereby providing a biological function for light-initiated adduct decay.

Further analysis of the flux dependence of the L:D ratio identifies two regimes that dictate the sensitivity of the LOV domain to changes in environmental light. Regime 1 occurs when k_T is large (phototropin-like), resulting in $k_T \sim k_R$ and broadening of the dependence of the L:D ratio on flux (Figure 5A,B). In this scenario, LOV proteins are sensitive over the entire dynamic range of biological actinic flux (Figure 5A,B). As

such, they are ideally suited for the measurement of gradients in light intensity, as needed for chloroplast localization and phototropism. In contrast, regime 2 (FKF1-like) is defined as $k_T \ll k_R$, where the L:D ratio is constant over all biologically relevant fluxes and determined directly from k_F/k_R (Figure 5B). In regime 2, the presence of light at dawn rapidly saturates the L:D ratio, even at fluence rates of $0.06 \mu\text{mol m}^{-2} \text{s}^{-1}$. These proteins are ideal for activating time-of-day specific responses such as the night–day transition. Importantly, the long lifetime of regime 2 proteins abolishes their ability to mark the day–night transition. Thus, the fast photocycle of ZTL may indeed be important for sensing biologically relevant actinic flux to determine the onset of dusk.

Examination of the fluence rate dependence of the L:D ratio for ZTL predicts the observed fluence dependence of ZTL mutants.²⁵ The lifetime positions the ZTL intermediate between regimes 1 and 2, allowing it to detect biologically relevant LL conditions (Figure 5B). Our model indicates that the light state of ZTL remains saturated from 10 to $600 \mu\text{mol m}^{-2} \text{s}^{-1}$ (82–86% light state). Below $10 \mu\text{mol m}^{-2} \text{s}^{-1}$, the L:D ratio rapidly decreases to 50% light at $1 \mu\text{mol m}^{-2} \text{s}^{-1}$, consistent with ZTL mutants that show pronounced effects below $10 \mu\text{mol m}^{-2} \text{s}^{-1}$.¹³ Importantly, the actinic flux 1 h prior to sunset is $\sim 6\text{--}12 \mu\text{mol m}^{-2} \text{s}^{-1}$. Thus, ZTL turnover will be initiated at dusk and proceed with first-order kinetics with a

time constant of 1.7 h. The lifetime allows more than four half-lives over an 8 h night, providing the maximal dynamic range in ZTL levels and providing a potential mechanism for measuring evening length in *A. thaliana*. Coupled with the function of FKF1s in measuring the onset of day, these proteins have evolved unique photochemical characteristics for potentially measuring day–night length in *Arabidopsis*.

Our kinetic model indicates spectral shifts in the light-state adduct may be important for tuning biological function. ZTL has an unusually blue-shifted light-state adduct (Figure 2D). Traditionally, the light state is characterized as S390, because of a traditional absorption maximum around 390 nm.²² ZTL is blue-shifted by 8 nm. Other proteins exhibit spectral shifts; for instance, the circadian clock photoreceptor VVD exhibits a mild red shift (Figure 2D). To the best of our knowledge, an effect of spectral shifts on biological function is currently not known. Interestingly, the intensity of actinic flux has large variances in the 380–410 nm range (Figure 2D). Thus, shifts in light-state spectra will have large effects on the rate of photoinitiated adduct scission, thereby affecting the L:D ratio. We examined the effect of the spectral shift of ZTL relative to VVD for its effect on L:D ratios. Here, we treat ZTL photochemistry ($\tau = 1.7$ h) with either the absorption profile of ZTL or that of VVD. The L:D ratio is significantly altered, resulting in a 30% decrease in the maximal L:D ratios and a decreased level of activation across the entire range of actinic flux.

Our kinetic model indicates that photoinduced adduct decay is required for biological detection of variances in actinic flux. These values must be considered in concert with thermal decay rate constants in designing variants to tune biological function and optogenetic tools. In addition, factors such as the spectral profile can have substantial effects on the light-state population under physiological lighting and must be considered when evaluating LOV domain variants.

DISCUSSION

LOV domain-containing proteins have been well studied because of their diverse function in biology and their ability to be manipulated for biotechnology purposes. An intriguing aspect of LOV domain chemistry has been the widely varying photocycle lifetimes. The natural variance of these lifetimes has been hypothesized to facilitate either adaptive or time-of-day specific functions, where adaptive responses required a short lifetime to allow resetting for a secondary response. The photocycle kinetics thus reflected an ability to be reset to changing levels of blue light. Treatment of LOV domains as light switches had neglected key aspects of their photochemistry.

Initial studies of LOV proteins identified a possible function as a photochromic switch, whereby blue-light activation could be reversed by subsequent absorption of UV-A light.²² The presence of UV light then induces formation of a photostationary state dependent on the presence of UV light (Figure S4 of the Supporting Information). Such chemistry has been exploited for biotechnology applications³⁴ but has not been examined in detail for biological function. Importantly, photoinitiated adduct decay has several implications for biological function. First, the ability to sense and adapt to both UV-A and blue light is particularly beneficial for differentiating among day, night, and cloud-cover conditions, where the relative contribution of UV-A to blue light will fluctuate. Such dual chromic sensing is reminiscent of the phytochromes, where plants use red and far-red light to

differentiate between shade and dark conditions.³⁵ Second, if UV-A light efficiently cleaves the adduct state, the adduct-state lifetime cannot be viewed as a timer mechanism. During daytime conditions, these proteins will be photodynamically switching between on (light-state) and off (dark-state) conditions regardless of the thermal adduct-state lifetime; therefore, these time scales are relevant only following nightfall.

Our kinetic model indicates that in the presence of photoinitiated adduct decay, the relative lifetime of the adduct state allows LOV domains to distinguish fluctuations in light intensity. In this regard, it provides a photochemical mechanism for the function of phototropins under low-flux conditions that remains sensitive to the entire dynamic range of blue light observed in nature. Such behavior has important consequences that can be exploited in improving our understanding of the biological mechanisms gating the photoreceptor function of LOV domains. For instance, pigment screening of light intensity will substantially affect the L:D ratio of functional protein depending on tissue depth. In this regard, the flux dependence of LOV domain function can allow discernment of tissues responsible for photoreceptor signaling.

Moreover, application of this model to circadian and photoperiodic timing in *A. thaliana* reveals that LOV domains likely tune diverse aspects of their photochemistry for specific biological function. Measurement of day length is difficult but imperative for plant survival. Utilization of two functionally related (FKF1 and ZTL) proteins with distinct fluence sensitivities allows a precise mechanism for day-length measurement. For instance, the long lifetime of FKF1 allows precise measurement of the onset of day through exquisite sensitivity to low flux. In contrast, an accelerated lifetime in ZTL allows low-flux sensitivity at dusk that can be coupled to thermal recovery at night to allow measurement of evening length. A similar gene network exists within the *Neurospora* circadian clock where VVD and WC-1 retain homologous LOV domains that are used in competitive dimer formation to regulate adaptation to changing levels of blue light.³⁶ Further characterization of these circadian clock photoreceptors will reveal if LOV domain photochemistry has evolved characteristics similar to those of ZTL/FKF1. Importantly, characterizations of ZTL, FKF1, and VVD are limited to their isolated LOV domains in the absence of their natural binding partners. Kinetic studies of full-length constructs in the presence and absence of their interaction partners will be required to construct a complete model of LOV domain function in these systems.

Importantly, gene duplication followed by evolutionary adaptation to function under specific fluence responses is common in plant photoreceptors. Both the phytochrome^{37,38} and phototropins³⁹ have homologues that specifically function under either LL or HL conditions. Previously, this has not been observed in the ZTL/FKF1/LKP2 family; rather, they were believed to behave similarly at the level of primary chemistry. Our kinetic model provides a simple framework for explaining how LOV domains can adapt to fluent responses through inclusion of the photocatalyzed rate constant. Moreover, it predicts evolutionary adaptation of ZTL to function at dusk, to measure day–night length in concert with FKF1. Further characterization of LOV domains may identify unique mechanisms of functioning as a light switch to measure varying degrees of light intensity to afford a biological advantage to organisms. Inclusion of photocatalyzed adduct scission in these

models allows researchers to use a new mechanism for tuning biological function or designing improved optogenetic devices.

■ ASSOCIATED CONTENT

■ Supporting Information

Kinetics of adduct decay under different sampling conditions (Figure S1), mono- and biexponential fitting with residuals of ZTL spectra (Figure S2), imidazole catalysis data for ZTL (Figure S3), and effect of UV light on adduct formation and scission (Figure S4). This material is available free of charge via the Internet at <http://pubs.acs.org>.

■ AUTHOR INFORMATION

Corresponding Author

*Department of Chemistry, Southern Methodist University, Fondren Science Building, Room 231, Dallas, TX 75275-0314. E-mail: bzoltowski@smu.edu. Phone: (214) 768-2640. Fax: (214) 768-4089.

Funding

This work was funded by the Herman Frasch Foundation (Grant 739-HF12 to B.D.Z.).

Notes

The authors declare no competing financial interest.

■ ACKNOWLEDGMENTS

We thank Jameela Lokhandwala for assistance with FKF1 data.

■ ABBREVIATIONS

LOV, light, oxygen, voltage; PAS, Period-Arnt-Single-minded; FMN, flavin mononucleotide; FAD, flavin adenine dinucleotide; ZTL, Zeitlupe; FKF1, Flavin-Kelch-Fbox-1; LKP2, LOV-Kelch-Protein-2; GI, Gigantea; TOC1, Timing Of Cab expression 1.

■ REFERENCES

- (1) Zoltowski, B. D., and Gardner, K. H. (2011) Tripping the Light Fantastic: Blue-Light Photoreceptors as Examples of Environmentally Modulated Protein-Protein Interactions. *Biochemistry* 50, 4–16.
- (2) Christie, J. M. (2007) Phototropin blue-light receptors. *Annu. Rev. Plant Biol.* 58, 21–45.
- (3) Crosson, S., Rajagopal, S., and Moffat, K. (2003) The LOV domain family: Photoresponsive signaling modules coupled to diverse output domains. *Biochemistry* 42, 2–10.
- (4) Ito, S., Song, Y. H., and Imaizumi, T. (2012) LOV domain-containing F-box proteins: Light-dependent protein degradation modules in *Arabidopsis*. *Mol. Plant* 5, 573–582.
- (5) Moglich, A., and Moffat, K. (2010) Engineered photoreceptors as novel optogenetic tools. *Photochem. Photobiol. Sci.* 9, 1286–1300.
- (6) Christie, J. M., Corchnoy, S. B., Swartz, T. E., Hokenson, M., Han, I.-S., Briggs, W. R., and Bogomolni, R. A. (2007) Steric Interactions Stabilize the Signaling State of the LOV2 Domain of Phototropin 1. *Biochemistry* 46, 9310–9319.
- (7) Raffelberg, S., Mansurova, M., Gartner, W., and Losi, A. (2011) Modulation of the photocycle of a LOV domain photoreceptor by the hydrogen-bonding network. *J. Am. Chem. Soc.* 133, 5346–5356.
- (8) Zoltowski, B. D., Nash, A. I., and Gardner, K. H. (2011) Variations in protein-flavin hydrogen bonding in a light, oxygen, voltage domain produce non-Arrhenius kinetics of adduct decay. *Biochemistry* 50, 8771–8779.
- (9) Zoltowski, B. D., Vaccaro, B., and Crane, B. R. (2009) Mechanism-based tuning of a LOV domain photoreceptor. *Nat. Chem. Biol.* 5, 827–834.
- (10) Chan, R. H., and Bogomolni, R. A. (2012) Structural water cluster as a possible proton acceptor in the adduct decay reaction of oat phototropin 1 LOV2 domain. *J. Phys. Chem. B* 116, 10609–10616.

- (11) Harmer, S. L. (2009) The Circadian System in Higher Plants. *Annu. Rev. Plant Biol.* 60, 357–377.

- (12) Moglich, A., Yang, X., Ayers, R. A., and Moffat, K. (2010) Structure and function of plant photoreceptors. *Annu. Rev. Plant Biol.* 61, 21–47.

- (13) Somers, D. E., Kim, W. Y., and Geng, R. S. (2004) The F-box protein ZEITLUPE confers dosage-dependent control on the circadian clock, photomorphogenesis, and flowering time. *Plant Cell* 16, 769–782.

- (14) Song, Y. H., Smith, R. W., To, B. J., Millar, A. J., and Imaizumi, T. (2012) FKF1 conveys timing information for CONSTANS stabilization in photoperiodic flowering. *Science* 336, 1045–1049.

- (15) Imaizumi, T., Tran, H. G., Swartz, T. E., Briggs, W. R., and Kay, S. A. (2003) FKF1 is essential for photoperiodic-specific light signalling in *Arabidopsis*. *Nature* 426, 302–306.

- (16) Kim, W. Y., Fujiwara, S., Suh, S. S., Kim, J., Kim, Y., Han, L. Q., David, K., Putterill, J., Nam, H. G., and Somers, D. E. (2007) ZEITLUPE is a circadian photoreceptor stabilized by GIGANTEA in blue light. *Nature* 449, 356–360.

- (17) Sawa, M., Nusinow, D. A., Kay, S. A., and Imaizumi, T. (2007) FKF1 and GIGANTEA complex formation is required for day-length measurement in *Arabidopsis*. *Science* 318, 261–265.

- (18) Mas, P., Kim, W. Y., Somers, D. E., and Kay, S. A. (2003) Targeted degradation of TOC1 by ZTL modulates circadian function in *Arabidopsis thaliana*. *Nature* 426, 567–570.

- (19) Lamesch, P., Berardini, T. Z., Li, D., Swarbrick, D., Wilks, C., Sasidharan, R., Muller, R., Dreher, K., Alexander, D. L., Garcia-Hernandez, M., Karthikeyan, A. S., Lee, C. H., Nelson, W. D., Ploetz, L., Singh, S., Wensel, A., and Huala, E. (2011) The *Arabidopsis* Information Resource (TAIR): Improved gene annotation and new tools. *Nucleic Acids Res.* 40, D1202–D1210.

- (20) Purcell, E. B., McDonald, C. A., Palfey, B. A., and Crosson, S. (2010) An analysis of the solution structure and signaling mechanism of LovK, a sensor histidine kinase integrating light and redox signals. *Biochemistry* 49, 6761–6770.

- (21) Kottke, T., Heberle, J., Hehn, D., Dick, B., and Hegemann, P. (2003) Phot-LOV1: Photocycle of a blue-light receptor domain from the green alga *Chlamydomonas reinhardtii*. *Biophys. J.* 84, 1192–1201.

- (22) Kennis, J. T. M., van Stokkum, N. H. M., Crosson, S., Gauden, M., Moffat, K., and van Grondelle, R. (2004) The LOV2 domain of phototropin: A reversible photochromic switch. *J. Am. Chem. Soc.* 126, 4512–4513.

- (23) ASTM Standard G173-03, 2012, Standard Tables for Reference Solar Spectral Irradiances: Direct Normal and Hemispherical on 37° Tilted Surface. ASTM International, West Conshohocken, PA, 2003, DOI: 10.1520/G0173-03R12.

- (24) Zikihara, K., Iwata, T., Matsuoka, D., Kandori, H., Todo, T., and Tokutomi, S. (2006) Photoreaction cycle of the light, oxygen, and voltage domain in FKF1 determined by low-temperature absorption spectroscopy. *Biochemistry* 45, 10828–10837.

- (25) Somers, D. E., Schultz, T. F., Milnamow, M., and Kay, S. A. (2000) ZEITLUPE encodes a novel clock-associated PAS protein from *Arabidopsis*. *Cell* 101, 319–329.

- (26) Harper, S. M., Neil, L. C., and Gardner, K. H. (2003) Structural basis of a phototropin light switch. *Science* 301, 1541–1544.

- (27) Herman, E., Sachse, M., Kroth, P. G., and Kottke, T. (2013) Blue-light-induced unfolding of the J α helix allows for the dimerization of aureochrome-LOV from the diatom *Phaeodactylum tricornutum*. *Biochemistry* 52, 3094–3101.

- (28) Zoltowski, B. D., Schwerdtfeger, C., Widom, J., Loros, J. J., Bilwes, A. M., and Crane, B. R. (2007) Conformational Switching in the Fungal Light Sensor Vivid. *Science* 316, 1054–1057.

- (29) He, Q., Cheng, P., Yang, Y., Wang, L., Gardner, K. H., and Liu, Y. (2002) White collar-1, a DNA binding transcription factor and a light sensor. *Science* 297, 840–843.

- (30) Alexandre, M. T., Arents, J. C., van Grondelle, R., Hellingwerf, K. J., and Kennis, J. T. (2007) A base-catalyzed mechanism for dark state recovery in the *Avena sativa* phototropin-1 LOV2 domain. *Biochemistry* 46, 3129–3137.

- (31) Jentzsch, K., Wirtz, A., Circolone, F., Drepper, T., Losi, A., Gartner, W., Jaeger, K. E., and Krauss, U. (2009) Mutual exchange of kinetic properties by extended mutagenesis in two short LOV domain proteins from *Pseudomonas putida*. *Biochemistry* 48, 10321–10333.
- (32) Schleicher, E., Kowalczyk, R. M., Kay, C. W., Hegemann, P., Bacher, A., Fischer, M., Bittl, R., Richter, G., and Weber, S. (2004) On the reaction mechanism of adduct formation in LOV domains of the plant blue-light receptor phototropin. *J. Am. Chem. Soc.* 126, 11067–11076.
- (33) Takemiya, A., Inoue, S., Doi, M., Kinoshita, T., and Shimazaki, K. (2005) Phototropins promote plant growth in response to blue light in low light environments. *Plant Cell* 17, 1120–1127.
- (34) Losi, A., Kottke, T., and Hegemann, P. (2004) Recording of Blue Light-Induced Energy and Volume Changes within the Wild-Type and Mutated Phot-LOV1 Domain from *Chlamydomonas reinhardtii*. *Biophys. J.* 86, 1051–1060.
- (35) Bae, G., and Choi, G. (2008) Decoding of light signals by plant phytochromes and their interacting proteins. *Annu. Rev. Plant Biol.* 59, 281–311.
- (36) Chen, C. H., DeMay, B. S., Gladfelter, A. S., Dunlap, J. C., and Loros, J. J. (2010) Physical interaction between VIVID and white collar complex regulates photoadaptation in *Neurospora*. *Proc. Natl. Acad. Sci. U.S.A.* 107, 16715–16720.
- (37) Casal, J. J., Sanchez, R. A., and Botto, J. F. (1998) Modes of action of phytochromes. *J. Exp. Bot.* 49, 127–138.
- (38) Neff, M. M., Fankhauser, C., and Chory, J. (2000) Light: An indicator of time and place. *Genes Dev.* 14, 257–271.
- (39) Harada, A., Sakai, T., and Okada, K. (2003) Phot1 and phot2 mediate blue light-induced transient increases in cytosolic Ca^{2+} differently in *Arabidopsis* leaves. *Proc. Natl. Acad. Sci. U.S.A.* 100, 8583–8588.